Iraqi Journal of Petroleum Geology and Geoinformatics Volume (0), Issue (0), Year (**2026**)
ISSN: 3105- 417X

Assessment of Soil Salinity and Suitability of Well Irrigation Water in Babylon, Iraq, Using Geomatics

Aurass Muhi Taha AL-Waeli[1]* and Israa Abdulqasim Mohammed Ali[1]
[1]*Department of Remote Sensing, College of Remote Sensing and Geophysics, Al-Karkh University of Science, Baghdad, Iraq.*

Abstract

Geomatics techniques provide a realistic quantitative and descriptive view of soil salinity, with the ability to spatially predict the suitability of well water for irrigation using Kriging. This procedure showed that 37.77% of the soils in the study area fall within the S0 soil class, which is not significantly affected by salinity. These are mostly agricultural soils located near surface water sources, meaning they rely on groundwater resources only during periods of severe drought and for a limited time. Additionally, the high percentage of morphologically non-saline soils (43.21%) is attributed to the presence of salt-tolerant field crop varieties within the lower limits of the S1 class. Saline areas are typically found at the edges of agricultural fields, adjacent to main and secondary drains. Soils affected by salinity and gradually transforming into slate are located in areas far from main irrigation canals and rely primarily on saline well water. This study concluded that only 42.66% of the moderately suitable water can be used in extreme necessity and during droughts, with the requirement for leaching. Soils when suitable good surface water is available. Poor and very poor ratios are a serious indicator of the possibility of salinization and degradation of the soils located above them. The unsuitability of this water for irrigation may be attributed to its higher salinity than its alkalinity due to the ionic composition of the groundwater with a high concentration of calcium and magnesium in limiting the activity of groundwater alkalinity.

1. Introduction

Human activity, particularly the unplanned use of water resources, contributes significantly to the deterioration of soil chemical properties. Salinity increases when a precise irrigation system is not followed, one that considers the quality of the water added to the soil. Dissolved ions in the water increase the salt concentration in the soil, while high sodium adsorption rates in this water raise soil sod levels. This negatively impacts soil quality and suitability for economically important plants, impacting countries' ability to maintain their economic and food security (Wu, et al, 2014). The harmful effect of chemical soil degradation on the agricultural environment is not limited to the use of water sources of unknown quality or the failure to carry out regular washing and drainage requirements, but also to the high addition of chemical fertilizers without resorting to organic fertilization, which causes disruption to the fertility balance in the soil(Mubarakah, and AL-Waeli, 2019), The decrease in the soil's organic matter content is a key indicator of chemical soil degradation when its salinity and sodity are within administratively controlled limits(AL-Waeli et al,2020). Soil information computing (geomatics) contributes to the development of current and future plans and studies for the sound management of soil and water resources. It also contributes to the inventory of agricultural or

* Email: aurasssoil@kus.edu.iq

degraded areas in the form of various maps or statistical diagrams. This is achieved when geological statistical methods are adopted in preparing these maps (AL-Waeli, 2020). Several studies have confirmed the possibility of preparing digital maps of different soil properties, by integrating laboratory tests of these properties with remote sensing data within predictive models and using multiple linear and non-linear regression formulas, with spatial accuracy that surpasses traditional maps (Taha et al, 2024). Because the duties of the soil and water resources surveyor are to be aware of the salinity of the soil and the role of well water suitability classes in accelerating this environmental phenomenon that threatens the soil resource, it has become necessary to adopt satellite data to diagnose the change in salt concentrations, as well as the morphological condition of the soil due to its change from the salinity-affected state to the shurah and then the sabkha, which is the stage of chemical desertification. This is achieved through documenting the spatial variation of soil salinity and water resources within the Geodatabase of Geographic Information Systems, especially those that contribute to meeting the goals of sustainable development in any agricultural country, especially in the dry regions of the world, by integrating field tests with laboratory analyses and remote sensing data, which contributes to the computerization of soil and water resource properties in the geomatics method(Kaplan, 2025). Geomatics techniques will be adopted in this study to prepare a predictive model integrating spectral indicators from remote sensing data with salt concentrations, to conduct a morphological classification of soil salinity using supervised classification technology, and to assess the suitability of well water in the study area for irrigation.

2. Materials and working methods

2.1 Location of the study area

The study area is located in central Iraq in the Babil Governorate, between latitudes 32°22'30.00"N to 33°18'40.00"N north and longitudes 44°29'30.00"E to 44°40'30.00"E east, within an area of 24,231 hectares.

2.2 Fieldwork

Twelve locations were identified for collecting well water samples with composite soil samples of a depth of 0-30 cm according to Lark, 2009 using a GPS device with a UTM coordinate system and were spatially projected onto a satellite image taken by the Landsat8 sensor on 12/16/2016, as shown in Figure 1.

2.3 Laboratory treatment of well water samples

Well water was filtered, and the electrical conductivity of the soil was measured using an EC-Meter and its reactivity using a pH-Meter, In addition, the dissolved calcium and magnesium were measured by titrating them with Na2-EDTA at a concentration of 0.01 N. Furthermore, the dissolved sodium and potassium were measured using a flame photometer according to (Estefan et al,2013). The sodium adsorption ratio in the well water was calculated using the following equation:

$$(SARw) = \frac{Na^{+}}{\sqrt{\frac{(Ca^{+2} + Mg^{+2})}{2}}} \quad (1)$$

In order to assess the suitability of well water for irrigation in the study area, and in addition to measuring salinity and sodium adsorption ratio, the percentage of dissolved sodium in groundwater was calculated from equation (2):

$$\text{Na}\ \% = \frac{(\text{Na}^{+}) + (K^{+})}{(Ca^{+2}) + (Mg^{+2}) + (\text{Na}^{+}) + (K^{+})} * 100 \qquad (2)$$

This is to achieve the classification mechanism within the scheme proposed by (Johnson and Zhang, 2009) and shown in Figure (2).

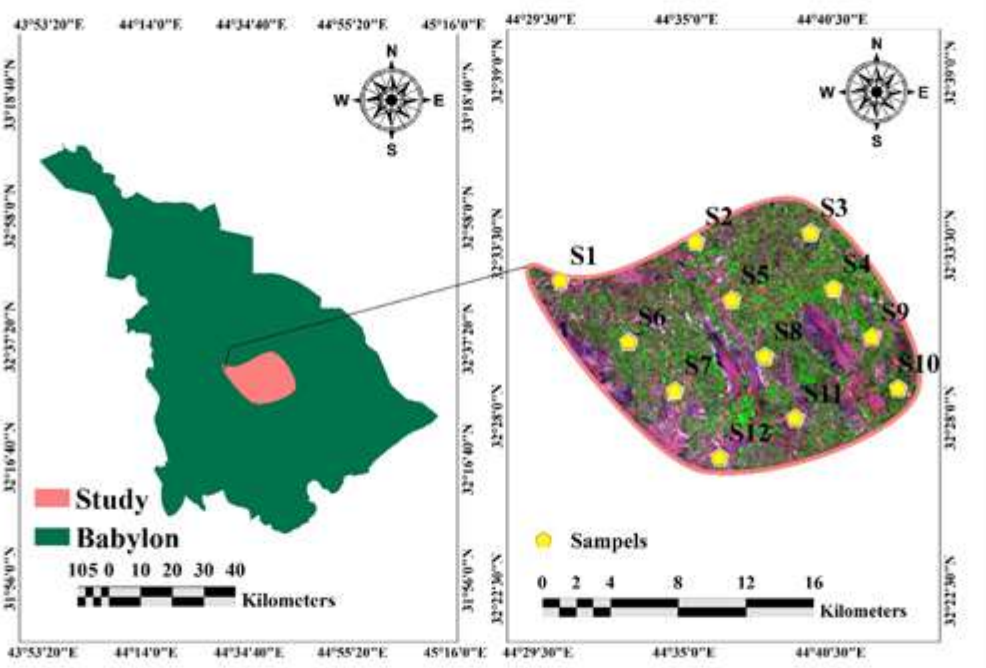

Figure 1: Shows the pattern of sample distribution in the study area.

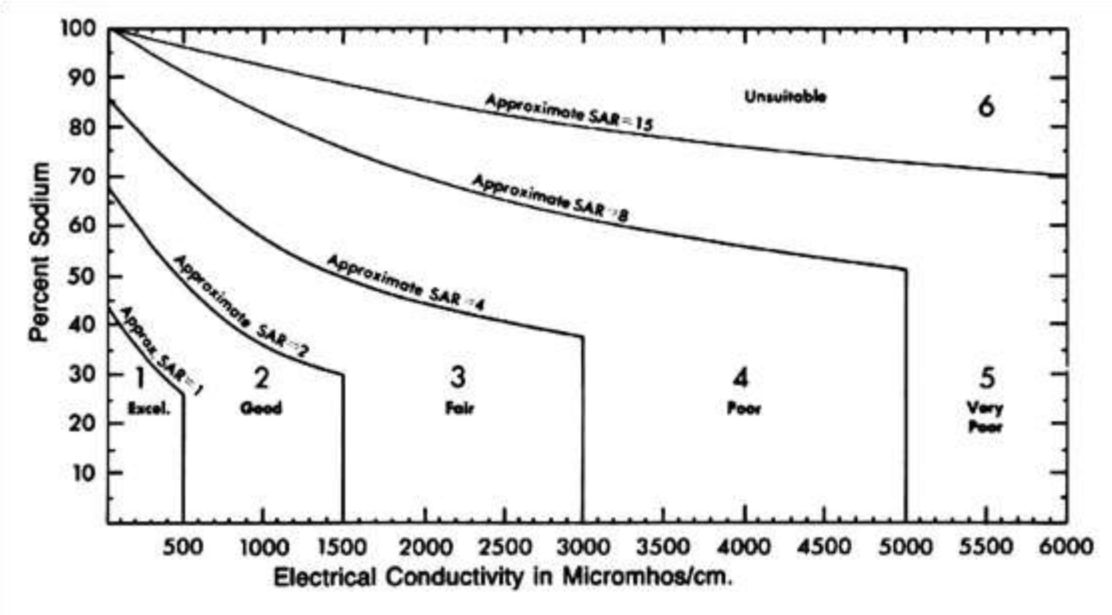

Figure 2: A diagram showing the classification of salinity, alkalinity, and suitability of groundwater for irrigation according to (Johnson and Zhang, 2009).

Table 1: Shows the results of laboratory analyses of well water.

Site	pHw	dS.m^{-1}	mmol.L^{-1}				Na%	SARw	Suitability	
		ECw	Ca	Mg	Na	K			Class	Value
S1	7.45	2.02	7.65	4.29	8.01	0.25	40.89	2.56	Fair	3
S2	7.47	1.85	7.43	4.05	6.81	0.21	37.95	2.21	Fair	3
S3	7.41	2.38	8.12	6.47	8.93	0.28	38.70	2.65	Fair	3
S4	7.02	3.33	9.35	12.22	11.38	0.35	35.23	2.89	Poor	4
S5	7.32	3.15	9.11	11.14	10.91	0.34	35.71	2.85	Poor	4
S6	7.45	2.03	7.66	4.36	8.03	0.25	40.79	2.56	Fair	3
S7	7.35	2.52	7.22	9.16	8.56	0.26	35.00	2.49	Fair	3
S8	7.37	2.72	8.56	8.53	9.81	0.30	37.17	2.74	Fair	3
S9	7.28	3.55	9.63	13.56	11.94	0.37	34.68	2.95	Poor	4
S10	7.13	4.82	8.77	28.8	10.31	0.32	22.05	2.14	Poor	4
S11	7.03	5.69	12.4	16.57	27.09	0.84	49.09	5.96	Very Poor	5
S12	7.19	4.26	10.55	17.86	13.76	0.43	33.31	3.12	Poor	4

2.4 Laboratory treatment of soil samples

The soil samples were air-dried at laboratory temperature, loosened, and passed through a 2 mm sieve. The laboratory measurements shown in Table 2 were performed. A saturated soil paste was prepared, and a soil solution was extracted. This solution was then filtered. The electrical conductivity of the soil was measured using an EC-Meter, and the degree of soil reaction was measured using a pH-Meter. In addition, the dissolved calcium and magnesium in the soil solution were measured by titrating them with Na_2-EDTA at a concentration of 0.01 N. Furthermore, the dissolved sodium and potassium in the soil solution were measured using a flame photometer according to (Estefan et al,2013) in order to calculate the sodium adsorption ratio in the soil from Equation (3):

$$(SARs) = \frac{Na^{+}}{\sqrt{\frac{(Ca^{+2}+Mg^{+2})}{2}}} \qquad (3)$$

Table 2: Shows the results of laboratory analyses of the measured soil properties.

Site	dS.m^{-1}	PHs	mmol.L^{-1}				SARs
	ECe		Ca	Mg	Na	K	
S1	2.52	7.73	8.88	4.39	11.48	0.45	4.46
S2	3.20	7.72	11.11	6.03	14.2	0.66	4.85
S3	5.14	7.71	17.25	14.58	19.04	0.53	4.77
S4	6.22	7.68	15.23	11.79	34.11	1.07	9.28
S5	3.80	7.71	10.55	6.37	20.51	0.57	7.05
S6	3.42	7.72	17.19	9.89	6.74	0.38	1.83
S7	5.41	7.69	21.69	17.63	14.09	0.69	3.18
S8	6.92	7.67	20.86	19.19	28.36	0.79	6.34
S9	10.89	7.42	31.44	38.96	37.46	1.04	6.31
S10	16.88	7.54	49.44	50.27	67.22	1.87	9.52
S11	21.18	7.48	51.33	60.01	97.75	2.71	13.10
S12	10.92	7.62	28.19	39.08	40.8	1.13	7.04

2.5 Soil properties diagnosis using remote sensing data

The image from the Landsat8 sensor was used, and its spectral bands were digitally processed according to the FLAASH (Fast Line of Sight Atmospheric Analysis of Spectral Hypercube) model. The study area was then cropped using ENVI 5.6. After conducting spatial fit tests, which achieve the most accurate representation of the soil properties under study, it was determined that the Generalized Difference Vegetation Index (GDVI2) is the most suitable for the predictive formulas, as shown in Equation (4), and is proposed by (Wu,2014):

$$\mathrm{GDVI}^2 = \frac{[(\mathrm{NIR})^2 - (\mathrm{Red})^2]}{[(\mathrm{NIR})^2 + (\mathrm{Red})^2]} \qquad (4)$$

It was calculated in ENVI 5.3 software, then its numerical values were extracted in ArcGIS software, and simple linear, logarithmic, and exponential regression analysis was performed on its numerical values with the soil salinity values measured in the laboratory within Microsoft Excel software, as shown in Figure 3:

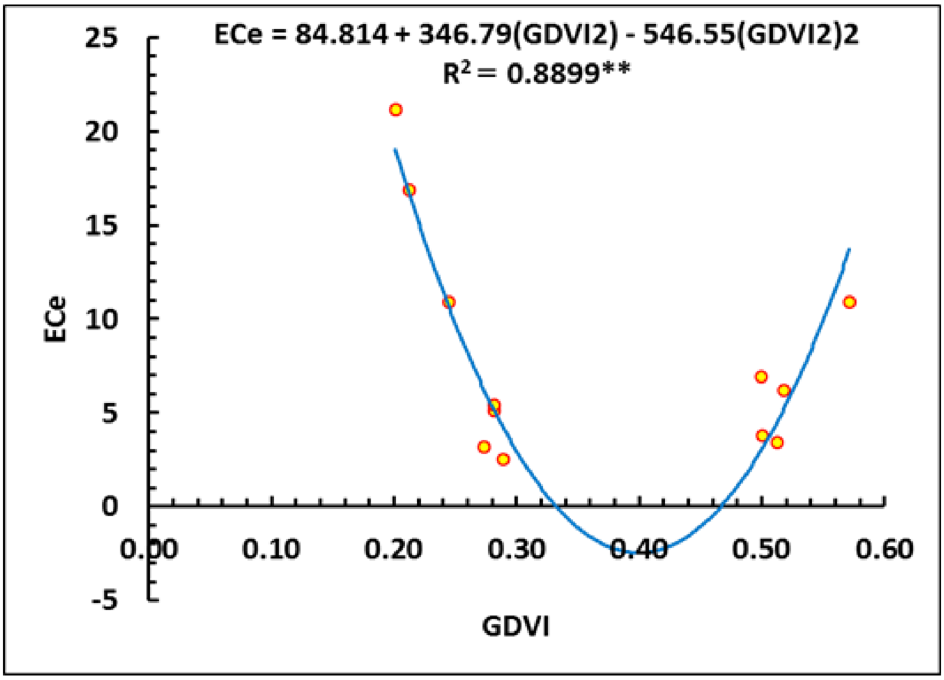

Figure 3: Predictive model of soil salinity from the exponential relationship with the spectral index GDVI.

Soil salinity was classified according to S.O.L.R., 1982, as shown in Table 3:

Table 3: Shows soil salinity classes according to S.O.L.R., 1982

Symbol	Class Description	EC $dS.m^{-1}$
S_0	Very Slightly Saline Soil	0 - 4
S_1	Slightly Saline Soil	4 - 8
S_2	Moderately Saline Soil	8 - 16
S_3	Strongly Saline Soil	16 - 25
S_4	Very Strongly Saline Soil	25 - 50
S_5	Extremely Saline Soil	> 50

2.6 Supervised classification

The numerical values in the space beams were converted to spectral reflectance ratios suggested, and the supervised classification was carried out in the ENVI 5.6 program to obtain the spectral signature of the land covers.

2.7 Spatial prediction of the hydrochemical properties of groundwater

The spatial prediction of the hydrochemical properties of the groundwater measured within the ArcGIS program was carried out according to the weighted variogram principle shown in Equation 5:

$$2\,\gamma(h) = \frac{1}{n(h)} \sum_{i=1}^{n(h)} [Z(x_i) - Z(x_i + h)]^2 \qquad (5)$$

Since a variable moves away from another variable by a spatial displacement of a certain amount, and using the Ordinary Kriging method within the ArcMap program, the Spherical Model shown in Equation (6) was applied to predict the salinity and suitability of groundwater for irrigation:

$$\gamma_{a,b}^{sph}(h) = \left\{ \begin{array}{c} b\left(\frac{3}{2}\frac{|h|}{a} - \frac{1}{2}\left(\frac{|h|}{a}\right)^3\right), if \;\; 0 \le |h| \le a \\ b\,, otherwise \end{array} \right\} \qquad (6)$$

The spatial prediction function of the spherical model ($\gamma_{a,b}^{sph}(h)$), where a represents the range and b represents the threshold for stability of the distance between the values of the spatial variable.

3. Results and Discussion

3.1 Quantitative Assessment of Soil Salinity

Figure 4 shows that 37.77% of the soils in the study area fall under the category of soils not significantly affected by salinity (S0).

These are mostly agricultural soils located near surface water sources, making their reliance on groundwater resources limited to periods of severe drought and for a short duration. Soils classified as saline (S1-S3) mostly rely on well water as the primary source for irrigation. This reflects the reality of water management in the soils of central and southern Iraq, given their location within an arid climate zone. Furthermore, the upstream countries of the Tigris and Euphrates rivers and their tributaries have reduced the water allocations granted to Iraq under international law. This means that surface water use in these soils is limited to short-term flood periods. Consequently, since the late 1980s, 60-70% of the total soils of central and southern Iraq have been lost due to salt accumulation, primarily resulting from the use of saline water sources with poor suitability for irrigation. (Wu et al, 2014), as for the two types S4 and S5, they practically represent soils outside the scope of agricultural use, and the current conditions indicate the possibility of expanding the area of these soils affected by salinity in the near future, and the continuous use of well water according to these current indicators will cause a major disruption in the salt balance in the soils of this region of Babylon Governorate, as AL-Waeli (2020) find that the reason for the activity of salt accumulation processes in arid regions with scarce water supplies and which depend on groundwater to a large extent is that they are more prone to secondary salinization, as the extraction of groundwater causes vertical drainage of the aquifer bearing salts, and with the absence of a system to drain it outside the soil body, it spreads into the deep groundwater, which in turn is used for irrigation, and this time with what it carries of salt compound ions, and over time it forms soils affected by salts and not economically productive.

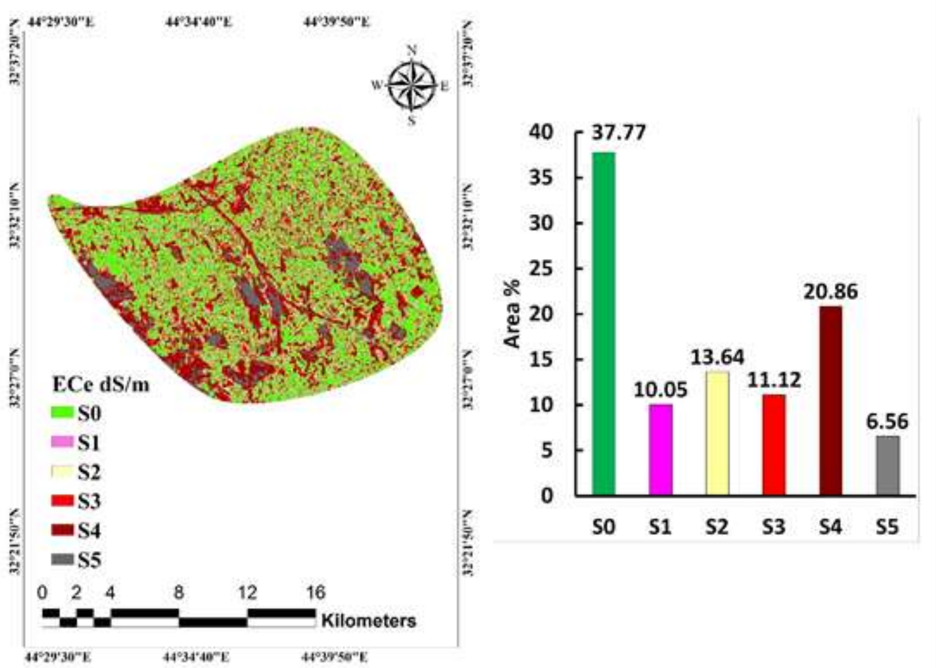

Figure 4: Distribution of soil salinity classes (quantitative state).

3.2 Descriptive Assessment of Soil Salinity

Figure 5 shows the spectral signature curves of the soil covers in the study area.

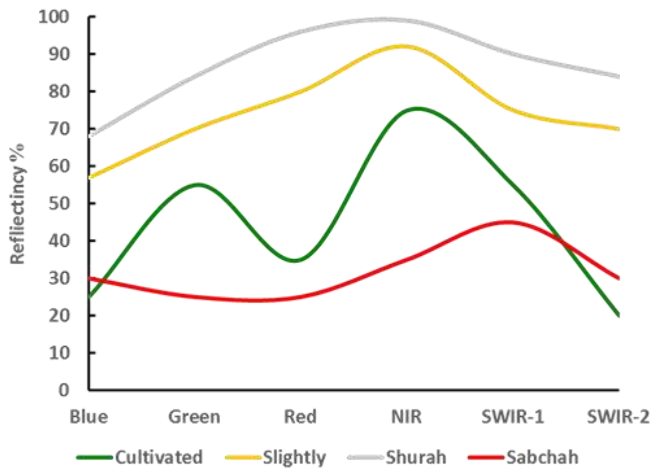

Figure 5: Spectral reflectance curves of saline soil types (descriptive case).

The spectral signature of soil salts varies depending on their mineral structure and their physicochemical behavior in nature in terms of color, shape, and extent of dispersion, as well as their ability to hydrate. It ranges from the white color of the salt crust that covers sodium chloride soils to the dark brown color of the swollen layer on the surface of calcium chloride soils (Taha et al,2024), There are six ranges in the electromagnetic spectrum that are useful in identifying the predominance of sodium chloride in saline and alkaline soils, extending from the visible spectrum to the mid-infrared. Sodium chloride exhibits the best absorption at 1400, 1900, and 2250 nm, while potassium chloride is identified at 1440 and 1933 nm, and magnesium chloride at 1190 and 1824 nm. Calcium chloride is difficult to distinguish due to its interaction with other salts. Gypsum is best absorbed at 1500–1730 nm, and sodium sulfate at 1978 nm. The reflectivity of saline soils varies depending on the type of salt, soil composition, and moisture conditions, making spectral identification an effective tool for classifying soil salinity(Metternicht and Zinck, 2003), Therefore, the categories shown in Figure (6) can be used to illustrate the descriptive state of soil salinity:

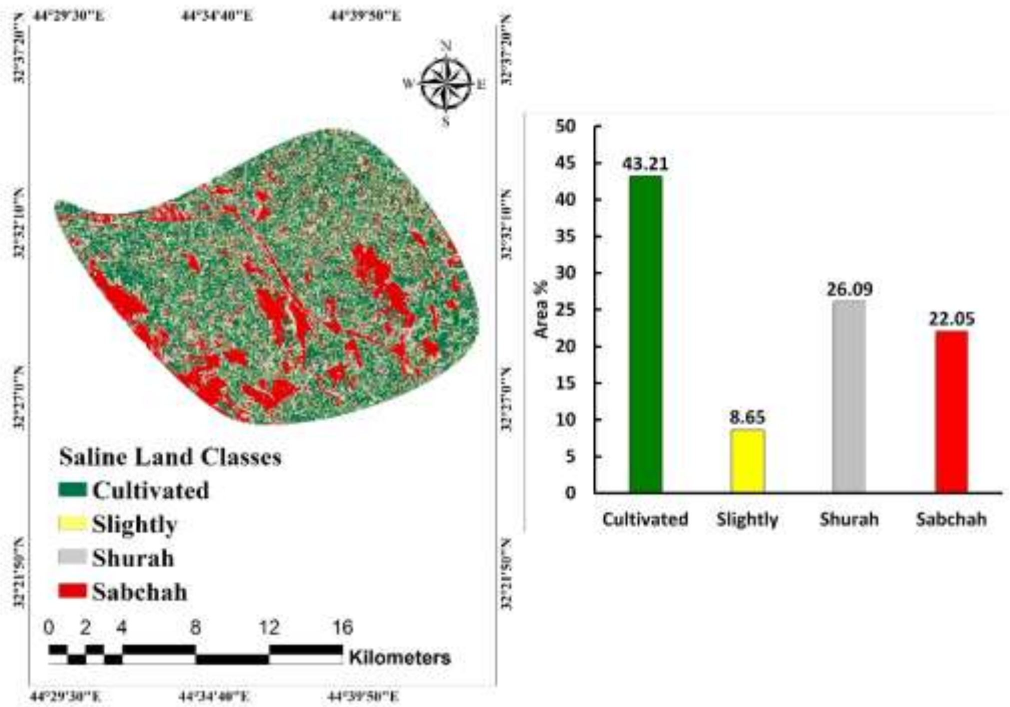

Figure 6: Soil salinity classes in the study area (descriptive case).

The high percentage of non-saline lands to 43.21% is attributed to the presence of salt-tolerant field crop varieties within the minimum limits of the S1 variety (Nezami and Alipour, 2012). Wu et al. (2014) found that barley grows within 6 decimans m-1. Saline areas are usually found at the ends of agricultural fields next to the main and secondary drains. As for the soils affected by salinity and gradually turning into sorghum, they are in areas far from the main irrigation canals and which depend mainly on saline well water (AL-Waeli and Al-Azawi, 2025).

3.3 Spatial Prediction of Well Water Suitability for Irrigation

Figure 7 shows that only 42.66% of moderately suitable water can be used in extreme necessity and during droughts, with the need to flush the soils when suitable surface water is available.

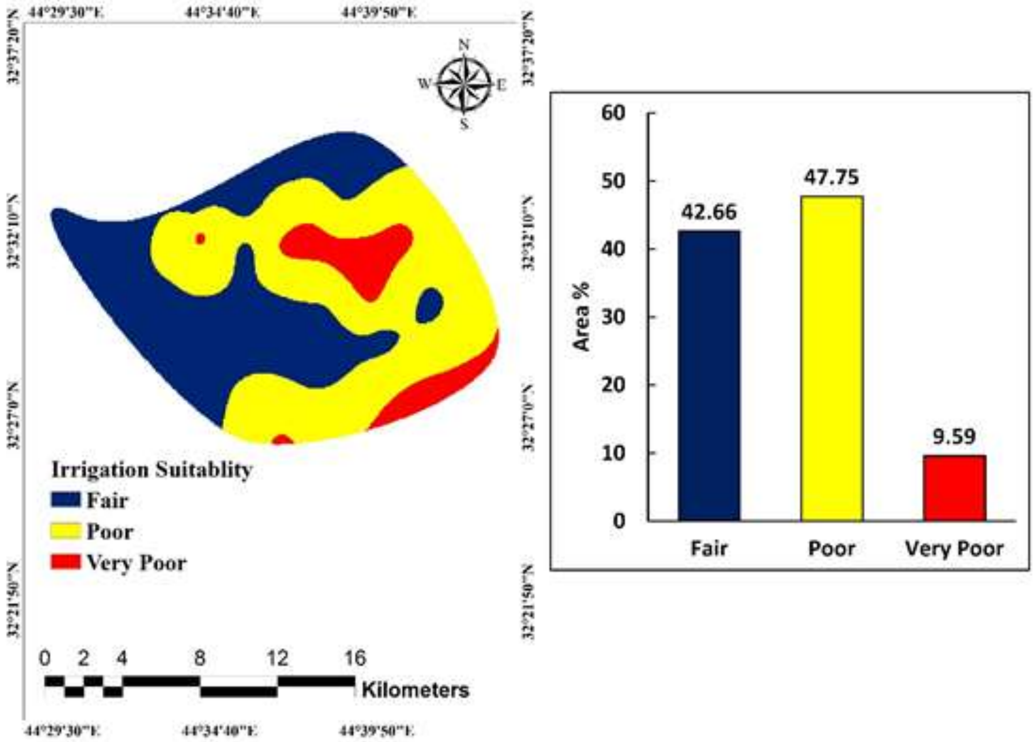

Figure 7: Classification of well water suitability in the study area.

Poor and very poor percentages are a serious indicator of the potential for salinization and degradation of the soils located above them. The unsuitability of this water for irrigation may be attributed to its higher salinity than its sodiness due to the ionic composition of the groundwater, with its high concentration of calcium and magnesium, which reduces the activity of groundwater sodiness. Al-Hurban and Al-Sulaimi (2009) showed that the ionic composition of groundwater with high concentrations of carbonates and magnesium plays a clear role in reducing sodiness activity due to the intense competition between magnesium and sodium for chlorides, which allows for the precipitation of a large amount of magnesium chloride salt. This explains the transformation of large areas of agricultural soils into saline soils with a morphological appearance characterized by darkness and a sticky texture(AL-Waeli et al,2024), The overlap of salinity and sodium indicators revealed a decrease in the area of good groundwater suitable for irrigation. Field surveys indicate a spatial correlation between poor groundwater quality and its location downstream of drainage networks and irrigation canal ends. These canals are often earthen and at lower elevations than their ideal design specifications due to haphazard dredging, allowing drainage water to seep into them. Furthermore, the unscientific mixing of drainage water with irrigation water in these canals contributes to the spread of highly concentrated salts to the upper aquifer, reducing its suitability for irrigation. Additionally, the seepage of sewage and industrial byproducts near urban centers into the groundwater further indicates a clear unsuitability based on all three indicators (AL-Waeli, 2020).

4. Conclusion

This study concluded the following:

1. It is possible to prepare quantitative and descriptive soil salinity maps using geomatics techniques.

2. It is possible to spatially predict the suitability of well water for irrigation using rigging.

This study also recommends the following:

1. Adopting this mechanism in preparing maps of different soil properties.

2. Developing an integrated program and models within ArcGIS software to understand the patterns of soil property distribution influenced by the surrounding environment or by the soil itself.

Conflicts of interest

The authors declare that there are no conflicts of interest regarding the publication of this study.

References

Al Waeli, Aurass Muhi Taha and Fadia W. Al-Azawi.(2.25). Geospatial Analysis of Management Indicators for Some Ghammas Soils in Integration with Sentinel Data. Sarhad Journal of Agriculture, 41(2): 946-957.

Al-Hurban , A . and J . S . Al-Sulaimi . (2009) . Recent surface sediments and landform of the southern area of Kuwait . European Journal of Scientific Research . 38 (2) : 272 – 295 .

AL-Waeli, A.M.T., 2020. Assessment of soil sensitivity for physical degradation in Abi- Garaq by geomatics techniques. Int. J. Agric.Stat. Sci., 16(Suppl. 1): 1865–1873.

Al-Waeli, A.M.T., F.W. Al-Azawi and H.M. Hamid. 2024. Evaluation of the sensitivity of Al-Husseiniya soils in Karbala to erosion using Landsat sensors. Environ. Challenges,

AL-Waeli, Aurass Muhi Taha, Samer Muhii Taha, and Saad Shakir Mahmood. (2020). Evaluation of drought impact on agricultural status for some Waist's soil using geomatic techniques. Plant Archives Vol. 20, Supplement (2) 554 – 565.

Estefan, G., R. Sommer and J. Ryan. 2013. Methods of soil, plant, and water nalysis: A manual for the West Asia and North Africa region. ICARDA. Third Edition.

Johnson, G. and H. Zhang. 2009. Classification of irrigation water quality. Oklahoma cooperative extension.

Kaplan, Fatma.(2025). Detection of Soil Salinity Using Remote Sensing and Machine Learning: Innovative Approaches and Contributions. MAS JAPS 10(1): 110 – 119.

Metternicht , G . I . and J . A . Zinck . 2003 . Remote sensing of soil salinity : potentials and constraints . Remote Sensing of Environment . 85 : 1 - 20 .

Mubarakah, Teeba M., and Aurass Muhi Taha AL Waeli. (2019). Evaluation of soil suitability for wheat using kriging and remote sensing data. Plant Archives. Vol. 19: 356 – 363.

Nezami , M . T . and Z . T . Alipour . 2012 . Preparing of the soil salinity map using geostatistics method in the Qazvin Plain . Journal of Soil Science and Environmental Management . 3(2) : 36 – 41 .

Taha, A.M., I.A. Ibrahim, H. Abduladeem, O.K. Ahmed, and T.N. Abdul-Allah. (2024). Assessing Drought Conditions in Southern Baghdad (1988–2023) Using NDVI Anomaly and Its Impact on Soil and Vegetation. Pakistan Journal of Agricultural Research. Vol. 37(3): 241 – 249.

Wu , W. (2014) . The Generalized Difference Vegetation Index (GDVI) for Dryland Characterization . Remote Sens. (6): 1211-1233.

Wu, Weicheng, Ahmad S. Mhaimeed, Waleed M. Al-Shafie, Feras M. Ziadat, Boubaker Dhehibi, Vinay Nangia, Eddy De Pauw. (2014). Mapping soil salinity changes using remote sensing in Central Iraq. Geoderma Regional, 2 – 3:21 – 31.